JEE Journal of Ecological Engineering

Journal of Ecological Engineering, 2027, 28(1), 144–154
https://doi.org/10.12911/22998993/241785
ISSN 2299–8993, License CC-BY 4.0

Received: 2026.09.06
Accepted: 2026.11.16
Published: 2026.12.01

Energy retention and pellet quality of water hyacinth after closed-loop vibrating torrefaction and binder-assisted densification

Montree Wongsiriwittaya[1*], Wirawut Lephon[1], Sanit Phinsakul[1]

[1] Faculty of Industrial Technology, Pibulsongkram Rajabhat University, 156 Moo 5, Phlai Chumphon, Mueang Phitsanulok, Phitsanulok 65000, Thailand
* Corresponding author's e-mail: montree.w@psru.ac.th

ABSTRACT

Transforming invasive water hyacinth into densified solid fuel offers a route to couple aquatic-weed management with renewable energy recovery. This study evaluated an integrated configuration combining temperature-controlled torrefaction in a vertically arranged, closed-loop vibrating reactor with downstream binder-assisted pellet densification. Raw biomass was washed, chopped to 10–20 mm, pre-dried to approximately 15% moisture, and torrefied at 240, 260, 280, 300, and 320 °C at a biomass feed rate of 300 g h^{-1}, with three independent runs at each temperature. Increasing torrefaction severity raised mean higher heating value (HHV) from 19.87 to 26.26 MJ kg^{-1} while mean solid yield declined from 85.33% to 59.27%. The trade-off was most pronounced above 300 °C: increasing temperature from 300 to 320 °C provided only a 0.98 MJ kg^{-1} HHV gain but caused an additional 6.86-percentage-point loss in solid yield. Product-side retained solid energy ranged from 15.56 to 16.95 MJ kg^{-1} of initial feed, and propagated uncertainty analysis showed that small differences among several conditions should be interpreted descriptively rather than as statistically demonstrated advantages. Pelletization improved physical handling characteristics. Binder-free pellets exhibited a pellet density of 979.14 ± 45.00 kg m^{-3}, a bulk density of 585.14 ± 35.00 kg m^{-3}, and mechanical durability of 93.15 ± 1.50%. Cassava starch produced the highest pellet density (1106.19 ± 35.00 kg m^{-3}), whereas used engine oil produced the highest bulk density (725.12 ± 85.00 kg m^{-3}). Mechanical durability increased to 97.20 ± 2.50% and 97.35 ± 5.50% with cassava starch and used engine oil, respectively, although both mean values remained slightly below the selected 97.5% reference benchmark. Accordingly, 260–300 °C is proposed as a promising development window under the investigated conditions rather than a validated process optimum. Because vibration intensity, process-gas flow, oxygen concentration, reactor energy consumption, combustion emissions, and contaminant behavior were not fully instrumented, the study does not claim a quantified reactor-performance advantage or demonstrated environmental superiority. Cassava starch is therefore the preferable tested binder when a bio-based formulation and high pellet density are prioritized.

Keywords: water hyacinth, torrefaction, vibrating reactor, biomass pellet, binder, retained solid energy, circular bioeconomy.

INTRODUCTION

Water hyacinth (*Eichhornia crassipes*) is an aggressive floating aquatic weed whose rapid proliferation can obstruct waterways, alter habitat structure, reduce dissolved oxygen, and create recurring costs for harvesting and disposal. Once removed from aquatic systems, however, the biomass also represents a lignocellulosic resource that can be redirected toward energy and material applications. Recent reviews therefore frame water-hyacinth management as a circular-bioeconomy challenge in which ecological removal, resource recovery, contaminant control, and value-added utilization should be considered together (Li et al., 2021; Bajpai and Nemade, 2023). More recent synthesis has further emphasized integrated biorefinery

pathways for valorizing harvested water hyacinth (Abba et al., 2025).

Direct use of aquatic biomass as a solid fuel is constrained by moisture, low bulk density, oxygen-rich organic matter, and comparatively high ash content. Torrefaction can reduce these limitations by driving dehydration, decarboxylation, decarbonylation, and partial decomposition of hemicellulose and other thermally labile fractions. The resulting solid is generally more carbon-rich and has a higher calorific value, but this improvement is accompanied by progressive mass loss as process severity increases (Cahyanti et al., 2020; Niu et al., 2019). Consequently, torrefaction should be evaluated as a mass-energy trade-off rather than by HHV alone. Temperature, residence time, reactor configuration, and feedstock properties all influence the balance between solid retention and fuel upgrading (Campbell et al., 2019; Kung et al., 2020).

Densification provides a complementary strategy because it increases volumetric fuel density and facilitates storage, transport, and feeding. Torrefaction, however, can reduce pelletability by degrading natural binding constituents and altering particle surface properties. Pilot-scale work has shown that torrefied biomass can achieve useful bulk densities but that mechanical durability remains strongly dependent on torrefaction severity, moisture, and press conditions (Agar et al., 2021). More broadly, moisture content, particle size, die geometry, temperature, pressure, and binder selection interact to determine pellet strength and process energy requirements (He et al., 2024; Sadeq et al., 2024).

Water-hyacinth pelletization has a comparatively narrow process window. Zhang et al. (2016) reported that moisture content and die temperature significantly affect pellet density and diametric compression strength. Other studies have demonstrated that combining thermal treatment with densification can improve hydrophobicity and modify pelletization energy demand (Chen et al., 2022; Yang et al., 2019). When torrefaction reduces natural binding capacity, external binders can improve particle bonding and pellet integrity; both solid and liquid additives have been investigated for thermally treated biomass (García et al., 2020; Butler et al., 2023).

Pellet quality is commonly assessed using physical indicators such as pellet density, bulk density, and mechanical durability. Historical fuel specifications, including DIN 51731 and EN 14961-2, have frequently been used as reference points for densified wood fuels (DIN, 1996, 2011). However, these standards were developed primarily for wood-derived densified fuels. The current ISO 17225-2:2021 applies to graded wood pellets, whereas ISO 17225-6:2021 covers graded non-woody pellets, including aquatic biomass; both exclude thermally treated biomass pellets from their respective scopes (International Organization for Standardization [ISO], 2021a, 2021b). Accordingly, the reference values adopted in the present study are used solely as comparative physical-quality benchmarks and should not be interpreted as evidence of formal fuel certification or full compliance with these standards.

Conventional torrefaction studies commonly employ fixed or slowly mixed beds under externally supplied inert gas, whereas the prototype evaluated here combines mechanical vibration with recirculation of non-condensable process gas. The intended engineering functions are repeated particle redistribution and heated-wall contact, together with reduced dependence on continuous external purge gas. However, the present project did not retain instrumented vibration frequency or amplitude, process-gas recirculation flow, oxygen concentration, or spatial temperature-profile data. Consequently, the study does not attribute the observed HHV or yield response quantitatively to vibration, nor does it claim superiority over conventional reactor designs. Its specific technical contribution is the integrated evaluation of temperature-dependent torrefaction, retained solid energy, and downstream binder-assisted pellet quality in this closed-loop vibrating configuration.

From an ecological-engineering perspective, valorization of harvested water hyacinth can reduce disposal burdens and create a potentially transportable solid fuel, but these benefits must be weighed against process electricity demand, combustion emissions, ash management, and possible contaminant transfer from waste-derived additives. Used engine oil is therefore evaluated here only as an experimental binder: trace metals, leaching behavior, ash chemistry, and combustion emissions were not measured. The present study focuses on three connected questions: (i) how torrefaction temperature changes the balance between solid yield and HHV; (ii) how much energy remains in the recovered solid after accounting for mass loss; and (iii) how cassava starch and used engine oil affect pellet density, bulk density, and mechanical durability. Unmeasured process-energy consumption and

environmental impacts are treated as future evaluation needs rather than demonstrated outcomes.

MATERIALS AND METHODS

Raw material preparation

Water hyacinth (Eichhornia crassipes) was harvested from local water bodies near Pibulsongkram Rajabhat University, Phitsanulok, Thailand. Soil and extraneous inorganic debris were removed by washing, after which the biomass was chopped into approximately 10–20 mm fragments. The prepared material was predried to a moisture content of approximately 15% before torrefaction to provide a consistent feed condition. The supplied project record identifies the collection area and preparation steps but does not preserve collection dates or a formal spatial/seasonal sampling design; these factors should therefore be considered when assessing feedstock representativeness.

Raw feedstock characterization

Proximate analysis, including volatile matter, fixed carbon, and ash content, was performed on a dry basis in accordance with ASTM D3172-13 and ASTM D3175-18 (ASTM International, 2013a, 2018). The higher heating value (HHV) of raw and torrefied samples was measured using a bomb calorimeter calibrated with benzoic acid in accordance with ASTM D5865-13 (ASTM International, 2013b). Ultimate analysis for carbon (C), hydrogen (H), nitrogen (N), and sulfur (S) was performed using a CHNS/O elemental analyzer. The ultimate-analysis results were expressed on a dry ash-free basis, and oxygen was calculated by difference as O (wt.%) = 100 – (C + H + N + S).

Experimental design

Torrefaction experiments were conducted across nominal reactor temperatures ranging from 240 to 320 °C (at 20 °C intervals) with a constant biomass feed rate of 300 g h^{-1}. Three independent runs were performed at each temperature level (n = 3 per temperature; 15 runs in total). Temperature served as the primary process-severity variable to evaluate solid yield and calorific-value enhancement. The recorded process time represents the observed transit time from biomass feeding to product discharge under each operating condition.

Vibrating reactor and closed-loop operation

The laboratory apparatus consisted of a vertically arranged vibrating torrefaction reactor integrated with a closed-loop gas-recirculation and condensation train. The system included electrical heating elements, thermal insulation, a motor-driven biomass feeder, temperature sensing and control, cyclone separation, electrostatic precipitation/condensation, water-assisted condensation, condensate collection vessels, gas-transfer piping, a circulation blower, a control valve, and a flow meter. Mechanical vibration was used to promote particle movement and redistribution within the heated reaction zone, while moisture and volatile products leaving the reactor passed through particulate and condensation stages. The remaining non-condensable gas was returned to the reactor through the blower and flow-control loop, a configuration intended to limit continuous ingress of ambient air and maintain a low-oxygen processing environment (Brachi et al., 2019). The same research group previously demonstrated circulating-gas torrefaction for lignocellulosic biomass in a related reactor context (Wongsiriwittaya et al., 2023).

For reproducibility, the measured operating variables available from the retained dataset are the nominal reactor set-point temperature, biomass feed rate, and observed feed-to-discharge transit time. The revision archive does not contain calibrated vibration frequency or amplitude, volumetric gas-recirculation rate, measured oxygen concentration, a spatial reactor-temperature profile, heating-rate history, or a residence-time distribution. These quantities are therefore not reconstructed or estimated retrospectively, and reactor-specific claims are limited to the documented operating configuration and measured product responses (Figure 1).

Pelletization and physical quality assessment

Torrefied water hyacinth was densified under three formulation categories: no binder, cassava starch binder, and used engine oil binder. Prior to densification, torrefied material was conditioned to approximately 15% moisture content and blended with either cassava starch or used

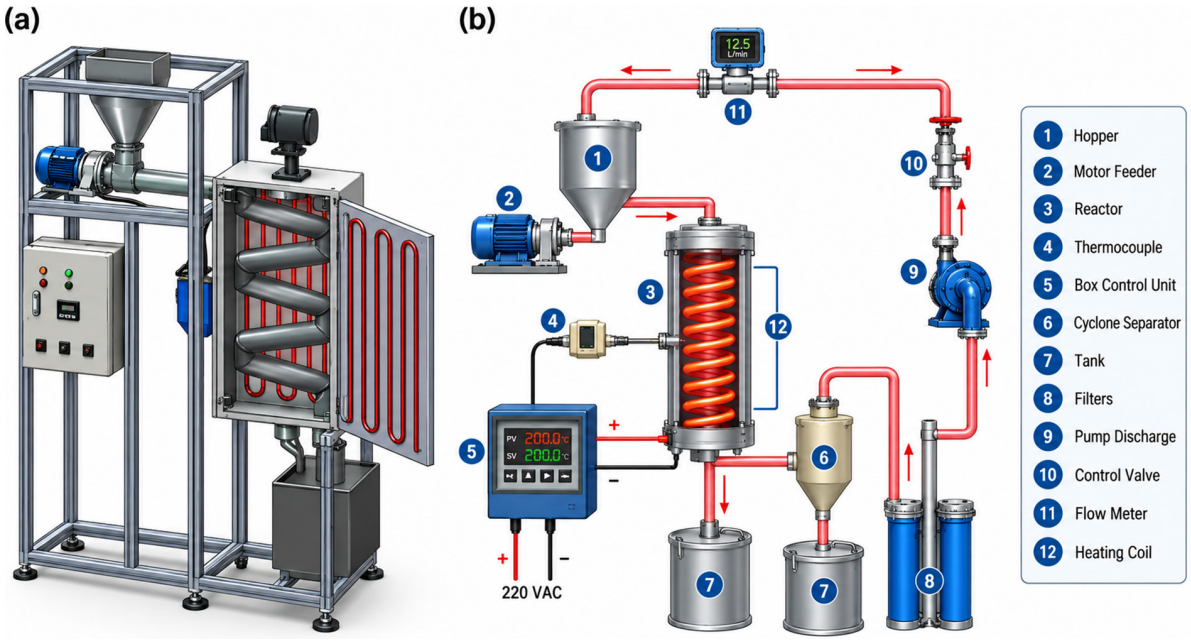

Figure 1. Vibrating reactor system: (a) 3D CAD model of the prototype assembly and (b) detailed schematic illustrating biomass feeding, electrically heated vibrating reactor, closed-loop gas recirculation, cyclone separation, electrostatic precipitator/condensation, and water-assisted condensation

engine oil at water-hyacinth-to-binder mass ratios of 90:10, 85:15, and 80:20 (w/w). Pellets were produced using a screw-type pelletizer equipped with a 6-mm die at approximately 80 ± 5 °C. The 80:20 water-hyacinth-to-used-engine-oil ratio exhibited the strongest energy-related response in its binder series, whereas 90:10 provided the highest HHV among the starch-containing formulations; these two formulations were therefore retained as representative binder conditions in the physical-quality comparison shown in Table 3.

Pellet density, bulk density, and mechanical durability were reported from the retained experimental dataset. For comparative interpretation, benchmark values of 1000 kg m^{-3} for pellet density, 600 kg m^{-3} for bulk density, and 97.5% for mechanical durability were used only as physical-quality reference points; they do not constitute evidence of formal compliance with DIN 51731, EN 14961-2, ISO 17225-2, or ISO 17225-6 because the tested material is thermally treated, non-woody aquatic biomass. The supplied revision files do not preserve a post-torrefaction particle-size distribution, quantitative mixing time/intensity, or the exact number of individual pellet specimens/technical repeats contributing to each mean ± SD in Table 3. These unrecorded procedural details are acknowledged as reproducibility limitations rather than retrospectively inferred.

Mass and energy calculations

Solid yield was calculated as $Y_s = (m_{tor}/mfeed) \times 100$, where m_{tor} is the mass of recovered torrefied solid and mfeed is the initial dry feed mass. Product-side retained solid energy was calculated as $Esolid = (Y_s/100) \times HHVtor$ and expressed in MJ kg^{-1} of initial feed. This metric represents the energy content retained in the recovered solid after torrefaction-induced mass loss and should not be interpreted as overall process energy efficiency because electrical energy consumed by the heater, vibration motor, blower, feeder, and auxiliary equipment was not measured. Descriptive uncertainty in Esolid was estimated by first-order propagation of the reported SDs for solid yield and HHV: $u(Esolid) = Esolid \times [(sY/Y)^2 + (sHHV/HHV)^2]^{1/2}$, assuming independent terms. The propagated value is used only to indicate calculation uncertainty; no inferential test was applied to Esolid.

To ensure a consistent energy baseline, relative energy densification ratio (EDR) for the binder-formulation dataset was recalculated as EDR = HHVproduct/HHVraw using the same untreated raw-feedstock mean HHV reported in Table 1, 15.80 MJ kg^{-1}. An EDR greater than 1 therefore indicates a higher gravimetric energy density than the untreated feedstock characterized in this study.

Statistical analysis

One-way ANOVA was conducted separately for process time, solid yield, HHV, pellet density, bulk density, and mechanical durability. For torrefaction responses, temperature was the treatment factor. For the physical pellet-quality comparison, the treatment factor comprised the three representative formulations shown in Table 3 (no binder, cassava starch 90:10, and used engine oil 80:20). Where significant treatment effects were identified, means were separated using Tukey's HSD test at $p < 0.05$. Analyses were conducted using IBM SPSS Statistics version 26. The archived statistical output supplied for this revision does not contain formal Shapiro-Wilk normality or Levene homogeneity-test results; therefore, the manuscript does not retrospectively claim that these diagnostics were completed. This documentation limitation is considered when interpreting marginal differences, particularly for pellet-quality outcomes.

RESULTS AND DISCUSSION

Baseline physicochemical characteristics

The raw feedstock exhibited the characteristics of an ash-rich aquatic biomass with a high volatile fraction and relatively low calorific value (Table 1). Volatile matter was 67.50 ± 4.20%, fixed carbon was 17.80 ± 3.50%, and ash was 14.70 ± 3.80%, giving a fuel ratio (FC/VM) of 0.264. The raw HHV was 15.80 ± 1.20 MJ kg^{-1}. Carbon, hydrogen, oxygen, nitrogen, and sulfur contents were 38.90 ± 3.50%, 5.30 ± 0.40%, 53.80 ± 4.00%, 1.80 ± 0.80%, and 0.18 ± 0.07%, respectively. The high volatile fraction supports rapid devolatilization, whereas the ash content reduces combustible-matter fraction and may become important during subsequent combustion. These baseline limitations provide the rationale for thermal upgrading before densification.

Temperature-driven torrefaction trade-off

Torrefaction temperature had a clear and opposing effect on calorific value and mass retention (Table 2 and Figure 2). One-way ANOVA indicated significant effects of torrefaction temperature on solid yield and HHV ($p < 0.05$). Mean HHV increased from 19.87 ± 0.23 MJ kg^{-1} at 240 °C to 26.26 ± 0.23 MJ kg^{-1} at 320 °C, whereas mean solid yield decreased from 85.33 ± 0.95% to 59.27 ± 0.76%. This response is consistent with progressive removal of moisture and oxygen-containing volatile products, which increases the relative concentration of the remaining solid fraction (Ibrahim et al., 2013; Singh et al., 2020). Similar temperature-dependent changes in solid yield and fuel quality are widely reported for biomass torrefaction (Cahyanti et al., 2020; Niu et al., 2019).

At 300 °C, the present HHV of 25.28 MJ kg^{-1} represents an increase of approximately 60% relative to the raw-feedstock mean of 15.80 MJ kg^{-1}. For comparison, Song and Kim (2013) reported an 8.18–30.04% heating-value increase during water-hyacinth torrefaction and a value of 4310.8 kcal kg^{-1} (approximately 18.04 MJ kg^{-1}) for washed material treated at 300 °C for 3 h. Pimchuai et al. (2010) likewise investigated water hyacinth among agricultural residues at 250–300 °C for 1–2 h in nitrogen and reported increasing energy density with torrefaction severity. The

Table 1. Proximate and ultimate analyses of raw water hyacinth feedstock. Proximate analysis is reported on a dry basis, whereas ultimate analysis is reported on a dry ash-free basis

Analysis	Parameter	Value (wt.% ± SD)
Proximate	Volatile matter (VM)	67.50 ± 4.20
Proximate	Fixed carbon (FC)	17.80 ± 3.50
Proximate	Ash	14.70 ± 3.80
Fuel property	HHV (MJ kg^{-1})	15.80 ± 1.20
Ultimate	Carbon (C)	38.90 ± 3.50
Ultimate	Hydrogen (H)	5.30 ± 0.40
Ultimate	Oxygen (O)	53.80 ± 4.00
Ultimate	Nitrogen (N)	1.80 ± 0.80
Ultimate	Sulfur (S)	0.18 ± 0.07
Derived	Fuel ratio (FC/VM)	0.264

higher 300 °C HHV observed in the present study should not be attributed solely to reactor vibration because feedstock ash content, pretreatment, residence time, reactor geometry, gas atmosphere, and analytical variability differed among studies.

The incremental benefit of higher temperature diminished above 300 °C. Raising the temperature from 300 to 320 °C increased HHV by only 0.98 MJ kg^{-1}, while solid yield fell by a further 6.86 percentage points. Thus, selecting 320 °C solely because it produced the highest HHV would ignore the associated loss of recoverable solid mass. Comparable studies have likewise shown that more severe thermal treatment can improve fuel quality while lowering material yield, emphasizing the need to optimize severity rather than maximize a single fuel-quality metric (Chen et al., 2020; Sui et al., 2024).

Retained solid energy and selection of a promising torrefaction window

Retained solid energy clarifies why the highest-HHV condition is not necessarily the most favorable condition for solid-fuel recovery. Across the temperature series, the calculated product-side energy content ranged from 15.56 to 16.95 MJ kg^{-1} of initial feed. The 240 °C condition had the highest mean-derived retained solid energy because of its high solid yield, while 300 °C retained 16.72 MJ kg^{-1} feed despite a substantially higher HHV. By contrast, 320 °C produced the maximum HHV but the lowest retained solid energy. The propagated uncertainty intervals overlap for several conditions; therefore, the numerical ordering of closely spaced retained-energy values is descriptive and should not be interpreted as a statistically significant ranking.

On the present data, 260–300 °C is best interpreted as a promising practical development window rather than a statistically optimized temperature range. At 260–280 °C, solid retention remains comparatively high but HHV enhancement is moderate; at 300 °C, calorific upgrading becomes substantial while mean retained solid energy remains comparable to the upper part of the observed range. The 320 °C condition adds little HHV relative to the additional mass loss. A full process-energy optimum cannot be identified because electrical demand of the heaters, vibration motor, blower, feeder, pumps, and controls was not measured. Process-simulation studies of integrated torrefaction and pelletization likewise show that auxiliary and thermal energy demand can materially influence system performance (Manouchehrinejad and Mani, 2019).

Binder-assisted pellet quality

Binder addition improved the mean values of all three measured pellet-quality indicators relative to the binder-free formulation (Table 3 and Figure 3). Binder-free pellets had a pellet density of 979.14 ± 45.00 kg m^{-3} and a bulk density of 585.14 ± 35.00 kg m^{-3}, both below the selected comparison thresholds, with durability of 93.15 ± 1.50%. Cassava starch increased pellet density by approximately 13.0% relative to the binder-free value and produced the highest pellet density, 1106.19 ± 35.00 kg m^{-3}. Used engine oil increased bulk density by approximately 23.9% relative to the binder-free value and produced the highest bulk density, 725.12 ± 85.00 kg m^{-3}. Durability increased by 4.05 and 4.20 percentage points with cassava starch and used engine oil, respectively. These differences are practically relevant for volumetric handling and mechanical integrity under the tested conditions, but they do not establish a general superiority of either binder across other feedstocks, pelletizers, or operating conditions.

Table 2. Statistical summary of water hyacinth torrefaction performance across operating temperatures

Temperature (°C)	Process time (min)	Solid yield (%)	HHV (MJ kg^{-1})	Retained solid energy (MJ kg^{-1} feed)
240	12.60 ± 0.57^{a}	85.33 ± 0.95^{a}	19.87 ± 0.23^{c}	16.95 ± 0.27
260	12.55 ± 1.45^{a}	79.10 ± 0.26^{b}	20.23 ± 0.08^{c}	16.00 ± 0.08
280	13.19 ± 2.02^{a}	70.60 ± 0.46^{c}	22.38 ± 0.45^{b}	15.80 ± 0.33
300	12.09 ± 0.04^{a}	66.13 ± 0.35^{d}	25.28 ± 0.40^{a}	16.72 ± 0.28
320	13.27 ± 0.18^{a}	59.27 ± 0.76^{e}	26.26 ± 0.23^{a}	15.56 ± 0.24

Note: Values for process time, solid yield, and HHV are mean ± SD (n = 3). Different lowercase superscripts within the same column indicate significant differences according to one-way ANOVA followed by Tukey's HSD test ($p < 0.05$). Retained solid energy is calculated from corresponding mean solid yield and mean HHV and is shown as mean-derived value ± first-order propagated uncertainty; it was not subjected to inferential statistical analysis.

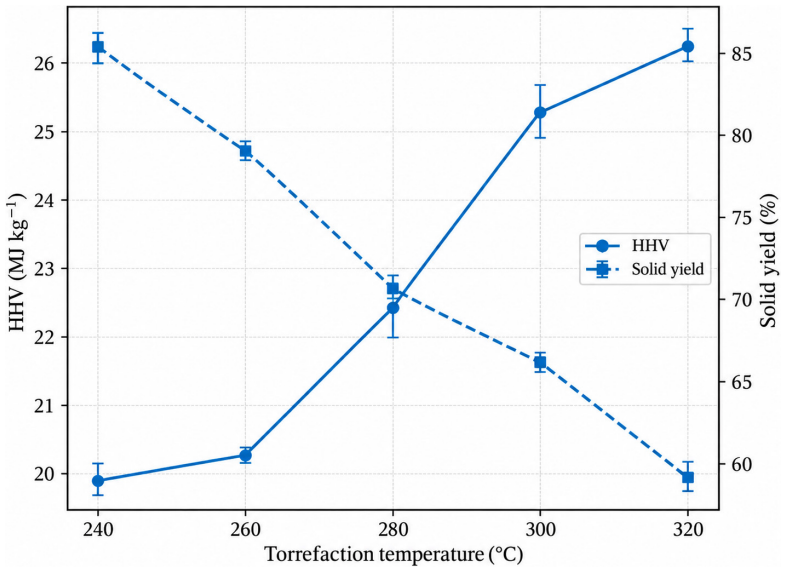

Figure 2. Temperature-driven trade-off between higher heating value (HHV) and solid yield during water-hyacinth torrefaction at 240–320 °C. Values represent mean ± SD (n = 3)

Cassava starch produced the highest pellet density, 1106.19 ± 35.00 kg m^{-3}, while also increasing bulk density to 689.19 ± 55.00 kg m^{-3} and durability to 97.20 ± 2.50%. Used engine oil produced a pellet density of 1026.12 ± 55.00 kg m^{-3} and the highest bulk density, 725.12 ± 85.00 kg m^{-3}, with durability of 97.35 ± 5.50%. The mean durability values for both binder-containing formulations remained slightly below the selected 97.5% reference benchmark; therefore, the observed improvement should not be interpreted as formal compliance.

Binder ratio affected fuel properties differently depending on binder type. For used engine oil, increasing the binder fraction progressively increased HHV, with the 80:20 formulation reaching 26.807 MJ kg^{-1} at 320 °C. In contrast, increasing cassava-starch content did not provide a corresponding energy benefit: the 90:10 starch formulation exhibited the highest HHV (21.663 MJ kg^{-1}), compared with 21.449 and 21.226 MJ kg^{-1} for the 85:15 and 80:20 formulations. When recalculated against the consistent 15.80 MJ kg^{-1} raw-feedstock baseline, relative EDR values were 1.548, 1.622, and 1.697 for the used-engine-oil series and 1.371, 1.358, and 1.343 for the cassava-starch series, respectively (Table 4).

The two binders therefore produced contrasting energy-response patterns. The hydrocarbon-rich oil increased gravimetric energy density as binder fraction rose, whereas additional starch beyond 10 wt.% provided no energy advantage under the tested conditions. This energy response does not, by itself, establish environmental acceptability of the used-engine-oil formulation. Its use would require independent evaluation of trace metals, combustion emissions, ash composition, and leaching behavior before any practical fuel recommendation.

Relative to the selected physical-quality benchmarks, the binder-free formulation remained below all three reference values. Both binder-assisted formulations exceeded the selected pellet-density and bulk-density benchmarks, whereas mean mechanical durability remained marginally below 97.5%. These comparisons indicate the degree of physical-quality improvement achieved by binder addition, but they should not be interpreted as formal compliance with commercial pellet standards. This distinction is particularly important because both ISO 17225-2:2021 for wood pellets and ISO 17225-6:2021 for non-woody pellets exclude thermally treated biomass pellets from their scopes.

Binder effects depend on particle wetting, lubrication, interparticle bonding, moisture, die conditions, and formulation; therefore, the observed performance should be treated as specific to the tested preparation conditions (Butler et al., 2023; He et al., 2024).

Engineering implications of the vibrating reactor and future energy assessment

The vibrating-reactor configuration provides a mechanistic rationale for maintaining particle motion and repeated wall contact during torrefaction without relying exclusively on high carrier-gas

Table 3. Physical and mechanical properties of binder-free and binder-assisted torrefied water-hyacinth pellets relative to selected physical-quality benchmarks

Formulation	Ratio (WH:binder)	Pellet density (kg m^{-3})	Bulk density (kg m^{-3})	Durability (%)
Selected reference benchmark	–	≥1000.00	≥600.00	≥97.50
No binder	–	979.14 ± 45.00^{c}	585.14 ± 35.00^{b}	93.15 ± 1.50^{b}
Cassava starch	90:10	1106.19 ± 35.00^{a}	689.19 ± 55.00^{a}	97.20 ± 2.50^{a}
Used engine oil	80:20	1026.12 ± 55.00^{b}	725.12 ± 85.00^{a}	97.35 ± 5.50^{a}

Note: Selected reference values are used solely as comparative benchmarks for physical pellet quality and do not indicate formal certification or full compliance with DIN 51731, EN 14961-2, ISO 17225-2, or ISO 17225-6. Values are presented as mean ± SD from the retained dataset. Different lowercase superscripts within the same column reflect the archived one-way ANOVA/Tukey HSD analysis ($p < 0.05$); formal normality/homogeneity diagnostic output and the exact number of individual pellet specimens were not available in the supplied revision archive.

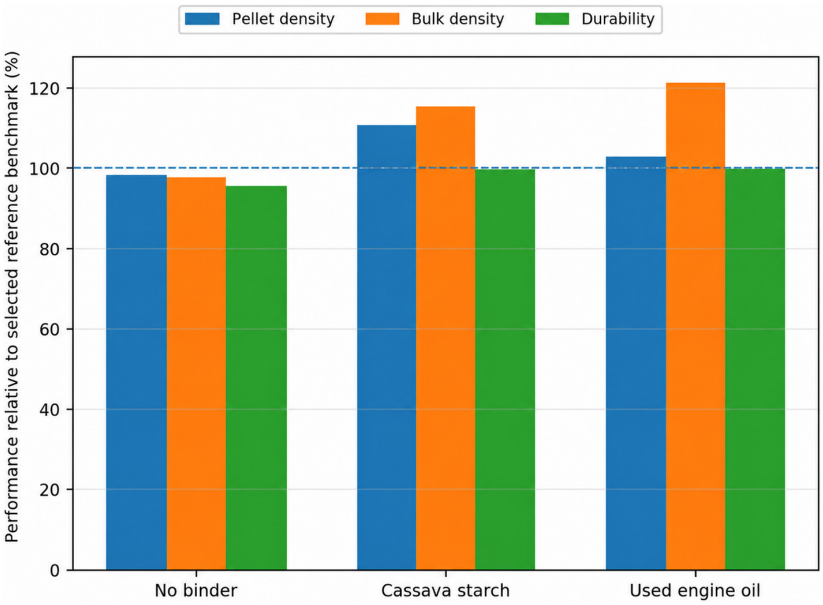

Figure 3. Normalized pellet density, bulk density, and mechanical durability of binder-free and binder-assisted torrefied water-hyacinth pellets relative to selected reference benchmarks of 1000 kg m^{-3}, 600 kg m^{-3}, and 97.5%, respectively. The horizontal line at 100% represents the corresponding reference benchmark.

flow, while gas recirculation can reduce the need for continuous external purge gas. In the present study, however, these potential advantages were not quantified against a non-vibrating control and cannot be separated from other reactor-configuration effects. Scale-up assessment should therefore include calibrated vibration frequency and amplitude, gas-flow and oxygen measurements, multi-point temperature logging, residence-time distribution, and a matched conventional-reactor comparison.

The net energy benefit likewise cannot be quantified from the retained dataset. Scale-up assessment will require separate metering of the electrical energy consumed by the heater, vibration motor, feeder, blower, pumps, and control system. Specific electrical energy consumption can then be calculated as $SEC = \Sigma(P_i t_i)/m_{product}$, expressed in kWh kg^{-1} or MJ kg^{-1} product.

Combustion performance should be validated experimentally rather than inferred from HHV alone. Recent work shows that torrefaction can alter ignition, flame stability, burn rate, and peak flame temperature, while ash behavior can influence deposition and sintering during pellet combustion (Bukhsh et al., 2026; Royo et al., 2025). Mechanical strength and combustion behavior of pellets containing industrial or waste-derived constituents also depend on formulation and ash chemistry (Dorokhov et al., 2024). Consequently, future co-firing evaluation should include combustion efficiency, gaseous emissions, particulate emissions, ash chemistry, and slagging or fouling indicators.

Table 4. Energy-related performance of selected binder formulations at 320 °C (EDR recalculated using the Table 1 raw-feedstock HHV baseline)

Binder	WH:binder ratio (w/w)	HHV (MJ kg^{-1})	Relative EDR
Used engine oil	90:10	24.460	1.548
Used engine oil	85:15	25.634	1.622
Used engine oil	80:20	26.807	1.697
Cassava starch	90:10	21.663	1.371
Cassava starch	85:15	21.449	1.358
Cassava starch	80:20	21.226	1.343

Note: Relative EDR = HHVproduct/HHVraw, using HHVraw = 15.80 MJ kg^{-1}, the untreated raw-feedstock mean reported in Table 1.

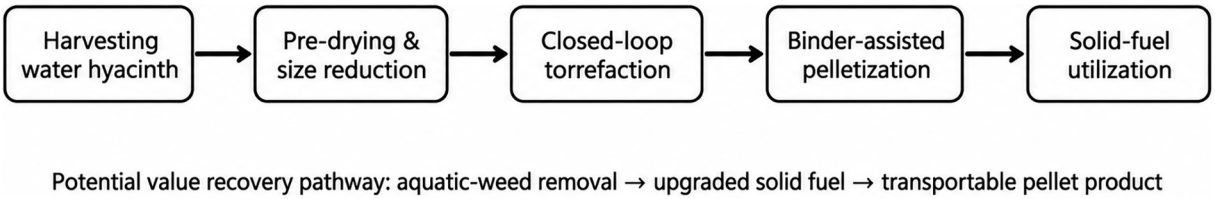

Figure 4. Conceptual potential circular-bioeconomy pathway linking water-hyacinth harvesting, feed preparation, closed-loop torrefaction, binder-assisted pelletization, and potential solid-fuel utilization The pathway is conceptual and does not represent a completed life-cycle assessment

Table 5. Potential multi-stage circular-economy accounting matrix and recommended evaluation indicators

Stage	Input	Output	Recommended indicator
Harvesting	Invasive water hyacinth	Biomass feedstock	kg dry feed per kg wet biomass
Torrefaction	Prepared biomass + process energy	Torrefied solid + vapors	Solid yield; HHV; retained solid energy; SEC
Pelletization	Torrefied solid + binder	Densified fuel	Pellet density; bulk density; durability
Energy use	Pellet	Heat + ash + emissions	Useful heat; combustion efficiency; emissions; ash behavior
Circularity	Biomass/waste streams	Potential value recovery	Material recovery; residue fate; contaminant transfer; life-cycle impacts

Potential circular-bioeconomy interpretation and limitations

The investigated process can be interpreted as a potential five-stage circular value chain – water-hyacinth harvesting, feed preparation, thermochemical upgrading, densification, and solid-fuel use (Figure 4; Table 5) – but the present experiments do not constitute a life-cycle or environmental-impact assessment. This framing is consistent with broader water-hyacinth valorization literature, which emphasizes that environmental benefit depends not only on producing a fuel but also on harvesting burden, conversion energy, residues, emissions, and downstream use (Li et al., 2021; Bajpai and Nemade, 2023).

Cassava starch is attractive where a bio-based binder is desired because it increased pellet density without introducing a petroleum-derived additive. Conversely, although used engine oil improved bulk density and durability in the present physical tests, its environmental suitability remains unverified. Contaminant transfer, trace-metal content, ash composition, leaching potential, and combustion emissions were not characterized. Accordingly, the used-engine-oil formulation is considered only an experimental waste-derived binder option and is not proposed for unrestricted fuel use.

CONCLUSIONS

Water-hyacinth torrefaction in the closed-loop vibrating reactor produced a clear temperature-dependent balance between fuel upgrading and solid retention. Mean HHV increased from 19.87 to 26.26 MJ kg^{-1} as temperature increased from 240 to 320 °C, while solid yield decreased from 85.33% to 59.27%. Increasing temperature from 300 to 320 °C yielded only 0.98 MJ kg^{-1} additional HHV but caused a further 6.86-percentage-point loss in solid yield. The maximum-HHV condition also had the lowest mean-derived retained solid energy (15.56 MJ kg^{-1} feed). On this evidence, 260–300 °C should be considered a promising operating/development window under the tested conditions rather than a definitive optimum; 300 °C provided substantial calorific upgrading without the additional mass penalty observed at 320 °C.

Binder-assisted densification improved the measured physical pellet properties. Cassava starch produced the highest pellet density (1106.19 ± 35.00 kg m^{-3}) and is the preferred tested formulation when a bio-based binder and high pellet density are prioritized. Used engine oil produced the highest bulk density (725.12 ± 85.00 kg m^{-3}), but its environmental suitability is not established because emissions, ash chemistry, trace metals, and leaching were not evaluated. Mean durability increased to 97.20 ± 2.50% with starch and 97.35 ± 5.50% with used engine oil, although both remained slightly below the selected 97.5% reference benchmark.

The principal technical contribution is the integrated assessment of torrefaction severity, retained solid energy, and binder-assisted pellet quality in a closed-loop vibrating-reactor configuration. The study does not establish overall process energy efficiency or a quantified advantage of vibration because reactor electricity use, vibration intensity, gas-flow/oxygen conditions, and a non-vibrating control were not measured. Future work should instrument these variables and directly evaluate combustion emissions, ash behavior, and contaminant fate before scale-up or environmental-performance claims are made.

Acknowledgements

The source research project was supported by the Science, Research and Innovation Promotion Fund (Fundamental Fund; Project Code: 208566).

REFERENCES

1. Abba, A., Sabarinath, S., Mustapha, R. A. (2025). Advancing circular bioeconomy through systematic review of multi-product biorefinery approaches for water hyacinth based renewable energy. *iScience, 28*(7), 112807. https://doi.org/10.1016/j.isci.2025.112807
2. Agar, D. A., Rudolfsson, M., Lavergne, S., Melkior, T., Da Silva Perez, D., Dupont, C., Campargue, M., Kalén, G., Larsson, S. H. (2021). Pelleting torrefied biomass at pilot-scale – Quality and implications for co-firing. *Renewable Energy, 178*, 766–774. https://doi.org/10.1016/j.renene.2021.06.094
3. ASTM International. (2013a). ASTM D3172-13: Standard practice for proximate analysis of coal and coke. ASTM International. https://doi.org/10.1520/D3172-13
4. ASTM International. (2013b). ASTM D5865-13: Standard test method for gross calorific value of coal and coke. ASTM International. https://doi.org/10.1520/D5865-13
5. ASTM International. (2018). ASTM D3175-18: Standard test method for volatile matter in the analysis sample of coal and coke. ASTM International. https://doi.org/10.1520/D3175-18
6. Bajpai, S., Nemade, P. R. (2023). An integrated biorefinery approach for the valorization of water hyacinth towards circular bioeconomy: A review. *Environmental Science and Pollution Research, 30*(14), 39494–39536. https://doi.org/10.1007/s11356-023-25830-y
7. Brachi, P., Chirone, R., Miccio, M., Ruoppolo, G. (2019). Fluidized bed torrefaction of biomass pellets: A comparison between oxidative and inert atmosphere. *Powder Technology, 357*, 97–107. https://doi.org/10.1016/j.powtec.2019.08.058
8. Bukhsh, K., Li, R., Ahmad, M. B., Zhao, Y., Hu, Z., Yue, S., Embaye, T. M., Li, X., Rahman, Z. U., Wang, X., Deng, S., Bai, Z. (2026). Comparative analysis of combustion behavior of raw and torrefied biomass pellets in a customized high-temperature flat flame furnace. *Fuel, 404*, 136301. https://doi.org/10.1016/j.fuel.2025.136301
9. Butler, J. W., Skrivan, W., Lotfi, S. (2023). Identification of optimal binders for torrefied biomass pellets. *Energies, 16*(8), 3390. https://doi.org/10.3390/en16083390
10. Cahyanti, M. N., Doddapaneni, T. R. K. C., Kikas, T. (2020). Biomass torrefaction: An overview on process parameters, economic and environmental aspects and recent advancements. *Bioresource Technology, 301*, 122737. https://doi.org/10.1016/j.biortech.2020.122737
11. Campbell, W. A., Coller, A., Evitts, R. W. (2019). Comparing severity of continuous torrefaction for five

biomass with a wide range of bulk density and particle size. *Renewable Energy, 141*, 964–972. https://doi.org/10.1016/j.renene.2019.04.057

12. Chen, D., Chen, F., Cen, K., Cao, X., Zhang, J., Zhou, J. (2020). Upgrading rice husk via oxidative torrefaction: Characterization of solid, liquid, gaseous products and a comparison with non-oxidative torrefaction. *Fuel, 275*, 117936. https://doi.org/10.1016/j.fuel.2020.117936
13. Chen, C., Yang, R., Wang, X., Qu, B., Zhang, M., Ji, G., Li, A. (2022). Effect of in-situ torrefaction and densification on the properties of pellets from rice husk and rice straw. *Chemosphere, 289*, 133009. https://doi.org/10.1016/j.chemosphere.2021.133009
14. Dorokhov, V. V., Nyashina, G. S., Romanov, D. S., Strizhak, P. A. (2024). Combustion and mechanical properties of pellets from biomass and industrial waste. *Renewable Energy, 228*, 120625. https://doi.org/10.1016/j.renene.2024.120625
15. DIN. (1996). DIN 51731:1996-10: Testing of solid fuels – Compressed untreated wood—Requirements and testing. Deutsches Institut für Normung.
16. DIN. (2011). DIN EN 14961-2:2011-09: Solid biofuels – Fuel specifications and classes—Part 2: Wood pellets for non-industrial use. Deutsches Institut für Normung.
17. García, R., González-Vázquez, M. P., Martín, A. J., Pevida, C., Rubiera, F. (2020). Pelletization of torrefied biomass with solid and liquid bio-additives. *Renewable Energy, 151*, 175–183. https://doi.org/10.1016/j.renene.2019.11.004
18. He, H., Wang, Y., Sun, Y., Sun, W., Wu, K. (2024). From raw material powder to solid fuel pellet: A state-of-the-art review of biomass densification. *Biomass and Bioenergy, 186*, 107271. https://doi.org/10.1016/j.biombioe.2024.107271
19. Ibrahim, R. H. H., Darvell, L. I., Jones, J. M., Williams, A. (2013). Physicochemical characterisation of torrefied biomass. *Journal of Analytical and Applied Pyrolysis, 103*, 21–30. https://doi.org/10.1016/j.jaap.2012.10.004
20. International Organization for Standardization. (2021a). ISO 17225-2:2021: Solid biofuels – Fuel specifications and classes–Part 2: Graded wood pellets (2nd ed.). ISO.
21. International Organization for Standardization. (2021b). ISO 17225-6:2021: Solid biofuels—Fuel specifications and classes—Part 6: Graded non-woody pellets (2nd ed.). ISO.
22. Kung, K. S., Thengane, S. K., Ghoniem, A. F. (2020). Functional mapping of torrefied product characteristics with index of torrefaction. *Fuel Processing Technology, 202*, 106362. https://doi.org/10.1016/j.fuproc.2020.106362
23. Li, F., He, X., Srishti, A., Song, S., Tan, H. T. W., Sweeney, D. J., Ghosh, S., Wang, C.-H. (2021). Water hyacinth for energy and environmental applications: A review. *Bioresource Technology, 327*, 124809. https://doi.org/10.1016/j.biortech.2021.124809
24. Manouchehrinejad, M., Mani, S. (2019). Process simulation of an integrated biomass torrefaction and pelletization plant to produce solid biofuels. *Energy Conversion and Management: X, 1*, 100008. https://doi.org/10.1016/j.ecmx.2019.100008
25. Niu, Y., Lv, Y., Lei, Y., Liu, S., Liang, Y., Wang, D., Hui, S. (2019). Biomass torrefaction: Properties, applications, challenges, and economy. *Renewable and Sustainable Energy Reviews, 115*, 109395. https://doi.org/10.1016/j.rser.2019.109395
26. Pimchuai, A., Dutta, A., Basu, P. (2010). Torrefaction of agriculture residue to enhance combustible properties. *Energy & Fuels, 24*(9), 4638–4645. https://doi.org/10.1021/ef901168f
27. Royo, J., Canalís, P., Quintana, D. (2025). Ash partitioning in combustion of pelletized residual agricultural biomass. *Biomass and Bioenergy, 193*, 107563. https://doi.org/10.1016/j.biombioe.2024.107563
28. Sadeq, A., Pietsch-Braune, S., Heinrich, S. (2024). Impact of press channel diameter-to-length ratio on the mechanical properties of biomass pellets during storage. *Fuel Processing Technology, 265*, 108149. https://doi.org/10.1016/j.fuproc.2024.108149
29. Singh, S., Chakraborty, J. P., Mondal, M. K. (2020). Torrefaction of woody biomass (*Acacia nilotica*): Investigation of fuel and flow properties to study its suitability as a good quality solid fuel. *Renewable Energy, 153*, 711–724. https://doi.org/10.1016/j.renene.2020.02.082
30. Song, D.-B., Kim, M. (2013). Characteristics of torrefaction with water hyacinth. *Journal of Biosystems Engineering, 38*(3), 180–184.
31. Sui, H., Chen, J., Cheng, W., Zhu, Y., Zhang, W., Hu, J., Jiang, H., Shao, J., Chen, H. (2024). Effect of oxidative torrefaction on fuel and pelletizing properties of agricultural biomass in comparison with non-oxidative torrefaction. *Renewable Energy, 226*, 120423. https://doi.org/10.1016/j.renene.2024.120423
32. Wongsiriwittaya, M., Chompookham, T., Bubphachot, B. (2023). Improvement of higher heating value and hygroscopicity reduction of torrefied rice husk by torrefaction and circulating gas in the system. *Sustainability, 15*(14), 11193. https://doi.org/10.3390/su151411193
33. Yang, Y., Sun, M., Zhang, M., Zhang, K., Wang, D., Lei, C. (2019). A fundamental research on synchronized torrefaction and pelleting of biomass. *Renewable Energy, 142*, 668–676. https://doi.org/10.1016/j.renene.2019.04.112
34. Zhang, X., Cai, Z., Chen, L., Zhang, D., Zhang, Z. (2016). Effects of moisture content and temperature on the quality of water hyacinth pellets. *BioResources, 11*(1), 1407–1416. https://doi.org/10.15376/biores.11.1.1407-1416